Cooperation of two-domain Ca^{2+} channel fragments in triad targeting and restoration of excitation–contraction coupling in skeletal muscle

Bernhard E. Flucher[†‡], Regina G. Weiss[§], and Manfred Grabner[§]

Departments of [†]Physiology and [§]Biochemical Pharmacology, University of Innsbruck, A-6020 Innsbruck, Austria

The specific incorporation of the skeletal muscle voltage-dependent Ca^{2+} channel in the triad is a prerequisite of normal excitation–contraction (EC) coupling. Sequences involved in membrane expression and in targeting of Ca^{2+} channels into skeletal muscle triads have been described in different regions of the α_{1S} subunit. Here we studied the targeting properties of two-domain α_{1S} fragments, green fluorescent protein (GFP)-I·II (1–670) and III·IV (691–1873) expressed alone or in combination in dysgenic (α_{1S}-null) myotubes. Immunofluorescence analysis showed that GFP-I·II or III·IV expressed separately were not targeted into triads. In contrast, on coexpression the two α_{1S} fragments were colocalized with one another and with the ryanodine receptor in the triads. Coexpression of GFP-I·II and III·IV also fully restored Ca^{2+} currents and depolarization-induced Ca^{2+} transients, despite the severed connection between the two channel halves and the absence of amino acids 671–690 from either α_{1S} fragment. Thus, triad targeting, like the rescue of function, requires the cooperation and coassembly of the two complementary channel fragments. Transferring the C terminus of α_{1S} to the N-terminal two-domain fragment (GFP-I·II·tail), or transferring the I–II connecting loop containing the β interaction domain to the C-terminal fragment (III·IV·βin) did not improve the targeting properties of the individually expressed two-domain channel fragments. Thus, the cooperation of GFP-I·II and III·IV in targeting cannot be explained solely by a sequential action of the β subunit by means of the I–II loop in releasing the channel from the sarcoplasmic reticulum and of the C terminus in triad targeting.

The majority of voltage-gated cation channels are composed of four homologous domains (repeats), each containing six membrane-spanning segments, including one voltage-sensing element and sequences contributing to the channel pore. K$^+$ channels are composed of four such domains expressed from separate transcripts. In Na$^+$ and Ca^{2+} channels the four homologous domains are connected in a single protein, the α_1 subunit (1). In the Ca^{2+} channel α_1 subunit the sequences flanking and connecting the four homologous repeats contain functional domains involved in the interaction with associated proteins and in channel targeting. The loop connecting repeats I and II of all high-voltage-activated Ca^{2+} channel α_1 isoforms carries the major β interaction domain (2). The association of the α_1 and the β subunit through this domain is important for membrane insertion and modulation of the channel (3–5). The loop connecting repeats II and III of the skeletal muscle α_{1S} isoform contains the sequence responsible for the bidirectional coupling of α_{1S} with the type 1 ryanodine receptor (RyR1). A 46-residue sequence within this loop is responsible for the Ca^{2+}-independent activation of the sarcoplasmic reticulum (SR) Ca^{2+} release channel (RyR1) in response to membrane depolarization (6). Conversely, the same sequence is necessary for the RyR1-dependent increase of Ca^{2+} conductance by the α_{1S} subunit (7). Sequences in the C terminus of the α_1 subunits are responsible for phosphorylation- and Ca^{2+}/calmodulin-dependent modulation of channel properties (8, 9). The C terminus also contains

secondary β interaction domains (10) and a signal important for the specific targeting of the α_1 subunit into the junctions between T-tubules and the SR, called the triads (11, 12).

With such important and unique functional domains located in the sequences flanking and connecting the homologous repeats it seems unlikely that, in analogy to the K$^+$ channels, fully functional Ca^{2+} channel α_1 subunits could be formed of multimers of single- or two-domain α_1 fragments. However, transcripts of two-domain Ca^{2+} channels have been found in muscle and brain (13–15), although their physiological role has not been determined. Individual expression of artificial two-domain fragments (I–II or III–IV) of α_{1S} did not restore Ca^{2+} conductance or excitation–contraction (EC) coupling in dysgenic myotubes, which lack the endogenous α_{1S} subunit (16). However, functional channels were expressed and EC coupling was restored when the two complementary fragments I–II and III–IV were coexpressed. Whereas restoration of skeletal muscle type EC coupling implies that the voltage-sensing α_{1S} subunit had been correctly targeted into the triad, it remained to be shown whether this was achieved by the incorporation of one or both channel fragments. Moreover, it was of interest to study whether either one of the fragments by itself can be targeted into the triad or whether the targeting process itself requires the interaction of both complementary channel fragments. To address these questions, we expressed two-domain fragments of α_{1S} separately and in combination in dysgenic myotubes and studied their triad-targeting properties. Because the two sequences known to be involved in membrane incorporation and triad targeting of α_{1S}—the β interaction domain in the I–II loop and the C-terminal triad-targeting sequence—are located in the I–II and III–IV fragments, respectively, we also tested composite two-domain constructs, each containing both of these sequences. The results presented here demonstrate that targeting and functional incorporation of the skeletal muscle Ca^{2+} channel into the triad requires the recombination of the complementary channel fragments and that the presence of the two known targeting domains in one channel fragment is not sufficient for the restoration of normal targeting functions.

Materials and Methods

cDNA Constructs. The cDNA coding sequences of the following rabbit skeletal muscle dihydropyridine receptor α_{1S} subunit constructs were inserted into the proprietary mammalian expression vector pGFP37 (17) either in-frame 3′ to the coding region of a modified green fluorescent protein (GFP) or into the same plasmid lacking the fluorescence tag (pGFP$^-$). Nucleotide numbers are given in parenthesis and asterisks indicate restric-

PHYSIOLOGY

tion enzyme (RE) sites introduced by PCR using the proofreading *Pfu Turbo* DNA polymerase (Stratagene).

GFP-I·II (α_{1S} 1–670). Two Stop codons (nucleotides 2011–2016) and a downstream positioned *Bam*HI* (nucleotide 2017) RE site were generated by PCR. The *Sph*I–*Bam*HI* fragment (nucleotides 1735–2017) of this PCR product was coligated with the *Sal*I–*Sph*I fragment (nucleotides −5–1735) of GFP-α_{1S} (17) into the corresponding *Sal*I/*Bam*HI polylinker RE sites of pGFP37.

III·IV (α_{1S} 691-1873). A *Xba*I* RE site (nucleotide 2057) upstream of nucleotides ACC (nucleotides 2062–2064) of a Met start codon (nucleotides 2065–2067) and of a codon for Glu (nucleotides 2068–2070) were introduced by PCR. The *Xba*I*–*Xho*I fragment (nucleotides 2057–2654) of this PCR product was coligated with the *Xho*I–*Eco*RI (nucleotide 2654–3′ polylinker) fragment of GFP-α_{1S} into the corresponding *Xba*I/*Eco*RI polylinker RE sites of pGFP⁻.

GFP-I·II·tail (α_{1S} 1–670-tail). cDNA coding for the C terminus of α_{1S} was fused to the α_{1S} 1–670 coding sequence at nucleotide 1984 by using the "gene SOEing" technique (18). The *Sph*I–*Bgl*II fragment (nucleotides 1735–4488) of the cDNA product generated by the fusion PCR was coligated with the *Sal*I–*Sph*I fragment (nucleotides −5–1735) of GFP-α_{1S} into the corresponding *Sal*I/*Bgl*II polylinker RE sites of pGFP37.

III·IV·βin (α_{1S} 691-1873-βin). cDNA coding for the III–IV loop of α_{1S} 691-1873 was replaced by I–II loop cDNA of α_{1S}. To this aim the *Xho*I–*Eco*RI* fragment (nucleotides 2654–3200) was coligated with an *Eco*RI–*Bgl*II fusion PCR fragment (nucleotides 1007–4488; transition site: 1296/3355) into the corresponding *Xho*I/*Bgl*II sites of α_{1S} 691-1873.

All sequences generated and modified by PCR were checked for integrity by sequence analysis (MWG Biotec, Ebersberg, Germany).

Cell Culture and Transfections. Myotubes of the homozygous dysgenic (*mdg*/*mdg*) mouse cell line GLT were cultured as described by Powell *et al.* (19). At the onset of myoblast fusion (2–3 days after addition of differentiation medium) GLT cultures were transfected by using the liposomal transfection reagent FuGene (Roche Diagnostics). Three to four days after transfection, myotubes were either fixed or used in physiological experiments. For electrophysiological recordings successfully transfected myotubes were identified by the fluorescence of the GFP fusion proteins or, in the case of the III·IV constructs, of GFP coexpressed from pure pGFP37.

Immunofluorescence Labeling. Differentiated GLT cultures were fixed and immunostained as described by Flucher *et al.* (20), using the monoclonal antibody 1A against the α_{1S} subunit (anti-α_{1S}) at a final concentration of 1:1,000 (21), a monoclonal or an affinity-purified anti-GFP antibody at 1:2,000 and 1:4,000, respectively (Molecular Probes), and the affinity-purified antibody no. 162 against the RyR1 at a dilution of 1:5,000 (22). Alexa-488-conjugated secondary antibodies were used with the anti-GFP antibodies so that the antibody label and the intrinsic GFP signal were both recorded in the green channel. Alexa-594-conjugated antibodies were used in double-labeling experiments to achieve a wide separation of the excitation and emission bands. Controls, for example the omission of primary antibodies and incubation with inappropriate antibodies, were routinely performed. Images were recorded on a Zeiss Axiophot microscope by using a cooled charge-coupled device camera and METAVIEW image-processing software (Universal Imaging, West Chester, PA). Quantitative analysis of the labeling patterns was performed by systematically screening the coverslips for transfected myotubes with a 63× objective.

Electrophysiological Analysis. Whole-cell patch-clamp recordings were performed with an Axopatch 200B amplifier controlled by PCLAMP 7.0 software (Axon Instruments, Foster City, CA). The bath solution contained 10 mM CaCl₂, 145 mM tetraethylammonium chloride, and 10 mM Hepes (pH 7.4 with tetraethylammonium hydroxide). Patch pipettes had resistances of 1.8–3 MΩ when filled with 145 mM cesium aspartate, 2 mM MgCl₂, 10 mM Hepes, 0.1 mM CsEGTA, 2 mM MgATP (pH 7.4 with CsOH). Depolarization-induced intracellular Ca^{2+} transients were measured during whole-cell recordings by including 2 mM tetrapotassium Fluo-4 (Molecular Probes) in the pipette solution. Currents were determined with 200-ms depolarizing steps from a holding potential of −80 mV to test potentials between −50 and +80 mV in 10-mV increments. Test pulses were preceded by a 1-s prepulse to −30 mV to inactivate endogenous T-type Ca^{2+} currents (23). Leak currents were digitally subtracted by a P/4 prepulse protocol. Recordings were low-pass Bessel filtered at 2 kHz and sampled at 5 kHz. Ca^{2+} currents were normalized by linear cell capacitance (expressed in pA/pF). After the recording of whole-cell Ca^{2+} currents, 0.5 mM Cd^{2+} and 0.1 mM La^{3+} were added to the external bath solution to enable the recording of immobilization-resistant intramembrane charge movement (gating currents; Q_{ON}) (23). The voltage dependence of Ca^{2+} conductance (G), charge movement (Q_{ON}), and intracellular Ca^{2+} release ($\Delta F/F$) was fitted according to a Boltzmann distribution $A = A_{max}/[1 + \exp(-(V − V_{1/2})/k)]$. A is G, Q_{ON}, or $\Delta F/F$; A_{max} is G_{max}, Q_{max}, or $(\Delta F/F)_{max}$; $V_{1/2}$ is the potential at which $A = A_{max}/2$; and k is the slope factor. Only currents with a maximal voltage error ≤10 mV attributable to series resistance were analyzed. All recordings were made at room temperature (≈23°C) and data are reported as mean ± SEM. Statistical significance was determined by unpaired Student's *t* test.

Results and Discussion

Association of Fragments I–II and III–IV Is Necessary for Triad Targeting. To analyze the ability of two-domain Ca^{2+} channel fragments to become targeted into the junctions between the SR and the T-tubules or the plasma membrane (for simplicity hitherto called triads), plasmids encoding residues 1–670 N-terminally fused to GFP (GFP-I·II) and residues 691-1873 (III·IV) of α_{1S} were generated. The split was placed early in the connecting loop between homologous repeats II and III. Similar to the two-domain fragments used in a previous study (16), the sequence 671–690, containing the so-called peptide A region with a postulated essential role for EC coupling (24), was omitted from the channel fragments.

Transfection and immunofluorescence labeling of dysgenic myotubes differentiated from the immortalized dysgenic cell line GLT (19) resulted in efficient expression of the two-domain channels fragments. Fig. 1 shows that on coexpression of GFP-I·II and III·IV the two complementary channel fragments were colocalized in clusters near the plasma membrane and throughout the myotubes. The characteristic labeling pattern and the colocalization with RyR1, which is expressed in the terminal cisternae of the SR, demonstrated that these clusters correspond to triad junctions (25). The rate at which the coexpressed two-domain fragments restored normal triad targeting in dysgenic myotubes was 73% (Table 1), which is even higher than previously reported for wild-type GFP-α_{1S} constructs (11). Thus, when expressed together, GFP-I·II and III·IV are both correctly targeted into skeletal muscle triads. In contrast, neither GFP-I·II nor III·IV expressed by itself was found in clusters colocalized with RyR1, but they were mainly localized in a cytoplasmic reticular structure corresponding to the developing ER/SR system (Fig. 1) (20). Functional analysis further under-
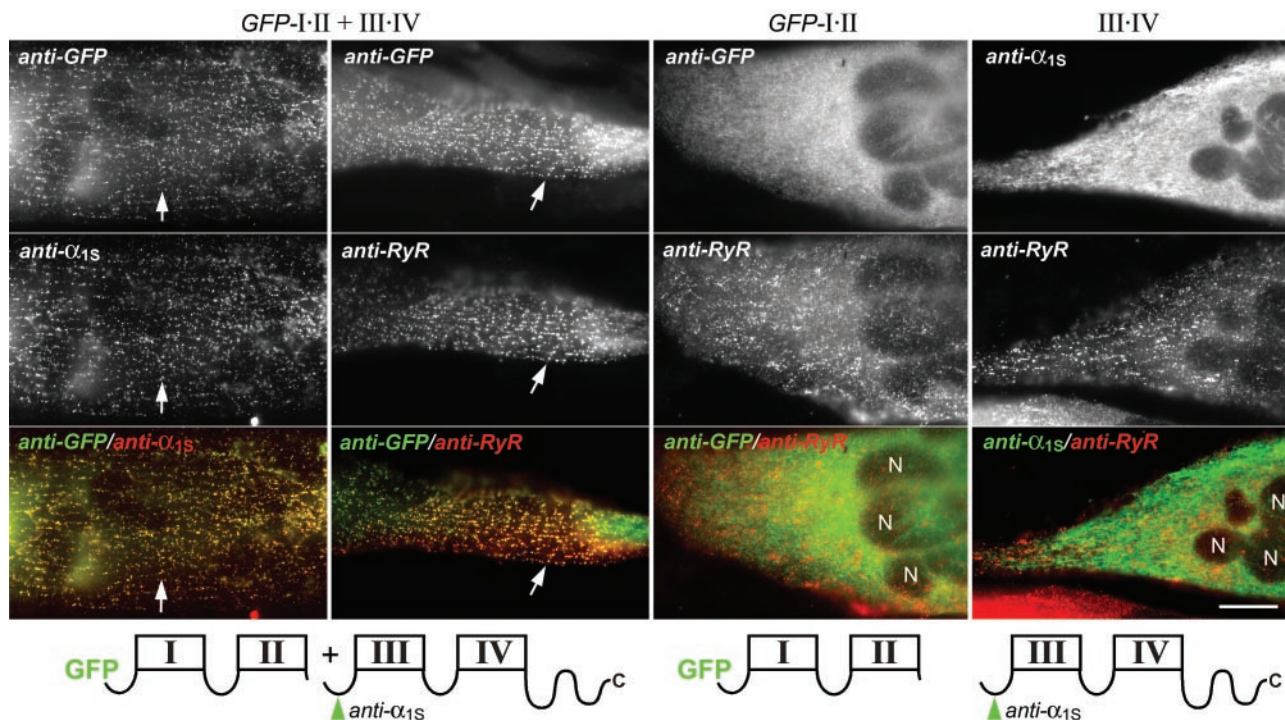
Fig. 1. Targeting properties of the two-domain Ca^{2+} channel fragments GFP-I·II and III·IV expressed in dysgenic myotubes. Transfected myotubes were double-immunofluorescence labeled with anti-GFP to detect GFP-I·II, anti-α_{1S} to detect III·IV (the locations of epitopes are indicated in green in the schematic drawings of α_{1S} fragments below the micrographs), and with anti-RyR as independent triad marker. When coexpressed, GFP-I·II and III·IV are colocalized with one another (first column) and with the RyR1 (second column) in clusters corresponding to triad junctions (examples indicated with arrows). Individually expressed GFP-I·II (third column) and III·IV (fourth column) are not colocalized with RyR1 clusters but are expressed throughout the endoplasmic reticulum (ER)/SR system. Merged color images (bottom row) of the micrographs above show colocalization of red and green fluorescent antibodies as yellow foci and lack of colocalization as separate red and green structures. The schematic drawings show the repetitive transmembrane domain structure of the α_{1S} fragments expressed in the myotubes shown above. N, nuclei. (Scale bar, 20 μm.)

scored these differential targeting properties of individually and combined two-domain α_{1S} fragments. In combination the complementary two-domain fragments reconstituted Ca^{2+} currents and EC coupling indistinguishable from wild-type GFP-α_{1S} (see below), whereas the individual constructs were unable to rescue either function. These observations are consistent with the findings of Ahern *et al.* (16). However, the present results further demonstrate directly that under conditions where EC coupling is restored (GFP-I·II + III·IV) actually both channel fragments are present in the triad junctions, and that GFP-I·II, which is expressed in the membrane but does not restore EC coupling, fails to be targeted

Table 1. Restoration of triad targeting by two-domain α_{1S} constructs expressed in dysgenic myotubes

Construct	% targeted myotubes*	No. of myotubes analyzed
GFP-α_{1S} (ref. 11)	58	967
GFP-I·II	0	361
III·IV	0	362
GFP-I·II + III·IV	73	735
GFP-I·II·tail	0	799
GFP-I·II·tail + III·IV	28	321
III·IV·βin	0	400
GFP-I·II + III·IV·βin	2	600

*Myotubes were classified as "targeted" if any region of the myotubes displayed the characteristic clustered immunolabeling pattern (see Fig. 1) colocalized with RyR1 label, which is indicative of triad labeling. The remainder represents myotubes in which the construct was expressed but not colocalized with RyR1-positive clusters.

into the triad. Thus, neither half of the Ca^{2+} channel α_{1S} subunit contains all of the information necessary for triad targeting of a two-domain channel fragment. The colocalization of GFP-I·II and III·IV in the triads suggests that the two fragments can recombine into a functional four-domain α_{1S} subunit, and that this recombination is necessary for normal targeting into the triads.

Triad Targeting Is Associated with Full Restoration of Ca^{2+} Currents and EC Coupling. The comparison of Ca^{2+} current and Ca^{2+} release properties of the coexpressed two-domain fragments with those of wild-type GFP-α_{1S} (Fig. 2) shows that voltage dependence, current density, and the amplitude of depolarization-induced Ca^{2+} transients were identical ($P > 0.05$). Moreover, all myotubes that showed depolarization-induced Ca^{2+} transients also displayed robust Ca^{2+} currents (Table 2). Ca^{2+} transients remained fully activated at voltages where Ca^{2+} currents approach the reversal potential (Fig. 2B), and blocking Ca^{2+} currents by the addition of Cd^{2+}/La^{3+} (not shown) did not block depolarization-induced Ca^{2+} transients. These characteristics demonstrate that the mode of EC coupling was independent of Ca^{2+} influx. Thus, coexpression of GFP-I·II and III·IV in dysgenic myotubes fully restores wild-type Ca^{2+} currents and Ca^{2+}-independent skeletal muscle-type EC coupling.

This is particularly important considering that the 20 amino acids (T671–L690) containing the peptide A region (24) were omitted at the boundary between the two channel fragments. In a previous study with similar two-domain fragments, Ca^{2+} currents were observed in only about one-quarter of all myotubes in which depolarization-induced Ca^{2+} release was measured and the current density was significantly reduced compared with full-length channel constructs (16). This finding had been inter-
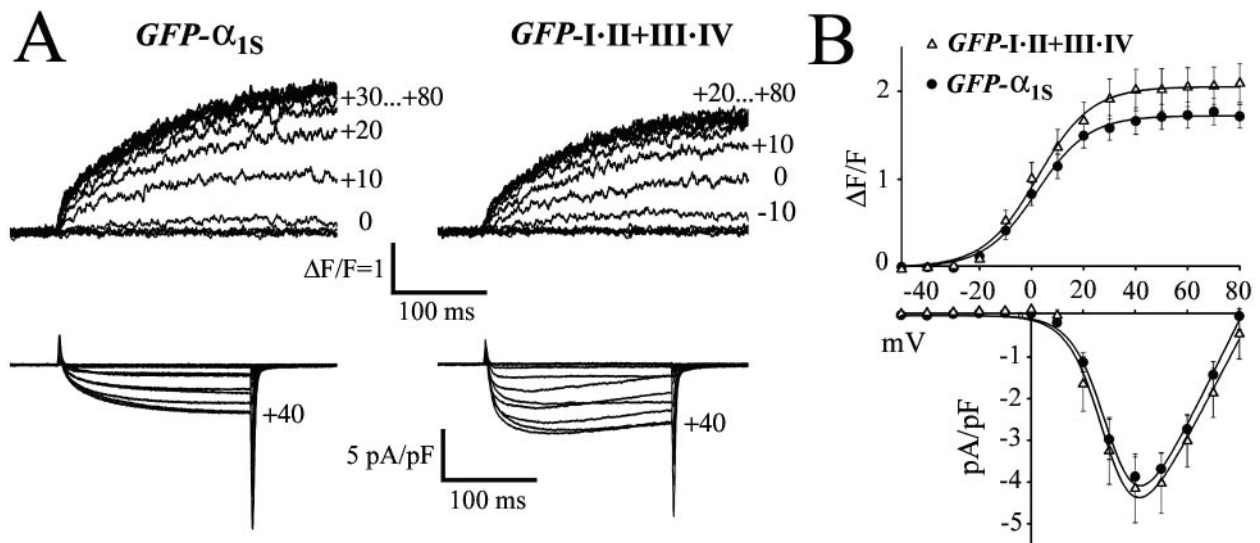
Fig. 2. Restoration of wild-type current densities and Ca^{2+} release properties by coexpression of complementary two-domain Ca^{2+} channel fragments in dysgenic myotubes. (A) Depolarization-induced Ca^{2+} transients (upper traces) and whole-cell Ca^{2+} currents (lower traces) recorded simultaneously from α_{1S}-null myotubes expressing wild-type GFP-α_{1S} or GFP-I·II + III·IV. The holding potential was −80 mV and 200-ms test pulses to potentials between −50 and +80 mV were applied in 10-mV increments. Changes in the cytoplasmic free [Ca^{2+}] were measured with Fluo-4 and shown as $\Delta F/F$. Apparent differences in activation and inactivation kinetics of I_{Ca} are within the normal range of variability and are not significantly ($P > 0.05$) different between wild-type and GFP-I·II + III·IV. (B) Comparison of the voltage dependence of depolarization-induced Ca^{2+} transients ($\Delta F/F$) and of peak Ca^{2+} current densities (pA/pF) recorded from α_{1S}-null myotubes expressing wild-type GFP-α_{1S} (●) and GFP-I·II + III·IV (△). Amplitudes of transient elevations of the cytoplasmic free [Ca^{2+}] and of the inward Ca^{2+} currents were identical ($P > 0.05$) for wild-type GFP-α_{1S} and coexpressed GFP-I·II + III·IV. Values represent the mean ± SEM of 9–14 recordings. The independence of Ca^{2+} transients from Ca^{2+} influx at voltages near the reversal potential (+80 mV) is characteristic of skeletal muscle EC coupling.

preted as failure of retrograde signaling from the RyR1 to the α_{1S} subunit, which normally causes the amplification of Ca^{2+} currents, because of the fragmentation of α_{1S} and/or the lack of the sequence 671–690. In light of our present finding that EC coupling and Ca^{2+} currents were fully restored by the fragmented α_{1S} subunit in all analyzed myotubes, this interpretation cannot be upheld. We find no evidence that RyR1-dependent amplification of Ca^{2+} currents is "unstable" (16). On the contrary, as previously shown for the fragmented Na^{+} channel (26), the pore function of the Ca^{2+} channel composed of GFP-I·II and III·IV was not compromised either. One possible explanation for the differences between the results of the two studies could be differences between the constructs used. Whereas the (PCR-

Table 2. Ca^{2+} conductance and Ca^{2+} transients obtained with two-domain α_{1S} constructs expressed in dysgenic myotubes

Construct	G_{max}, nS/nF	Ca^{2+} transient, ($\Delta F/F$)$_{max}$	No. of myotubes analyzed
GFP-α_{1S}	138 ± 11.3	1.7 ± 0.1	14
GFP-I·II	—	—	6
III·IV	—	—	5
GFP-I·II + III·IV	132.1 ± 15.3*	2.1 ± 0.2*	9
GFP-I·II·tail	—	—	7
GFP-I·II·tail + III·IV	166.5 ± 21.3*	0.9 ± 0.2†	7
III·IV·βin	—	—	5
GFP-I·II + III·IV·βin	193.5 ± 30.5*	1.8 ± 0.5*	6

G_{max} is the maximal Ca^{2+} conductance. ($\Delta F/F$)$_{max}$ are maximal depolarization-induced Ca^{2+} transients. Data are given as mean ± SEM. Currents and transients are fitted to a Boltzmann distribution. Constructs exhibiting no detectable L-type Ca^{2+} currents (<10 pA) and Ca^{2+} transients (<0.1 $\Delta F/F$) are indicated with —.
*Values are not statistically significant different from those of wild-type GFP-α_{1S} ($P \geq 0.05$).
†Ca^{2+} transients are significantly lower than those of GFP-α_{1S} ($P < 0.005$).

introduced) start codon of our fragment III·IV is in the context of a consensus sequence for the initiation of translation (AC-CatgG) (27) identical to the wild-type α_{1S} subunit, the corresponding construct of Ahern et al. (16) supposedly starts at an internal methionine (M701) codon preceded by 12 codons for native II–III loop residues. Another possible source of the different results could be the cell system. In our hands GLT dysgenic myotubes developed a much higher density of triads than did primary dysgenic myotubes (cf. refs. 19 and 20).

GFP-I·II or III·IV expressed alone did not restore Ca^{2+} conductance or EC coupling in dysgenic myotubes (Table 2). But in agreement with Ahern et al. (16), considerable values of intramembrane charge movement (gating charge) could be recorded from cells expressing GFP-I·II alone. The value of Q_{max} was 5.1 ± 1.1 nC/μF ($n = 6$), which is close to the 6.8 ± 0.5 nC/μF ($n = 13$) recorded from wild-type GFP-α_{1S} (28). Charge movement comparable to wild-type levels is indicative of substantial membrane expression of this two-domain fragment. Since no triad targeting and little or no membrane labeling could be observed with this construct, it is probably diffusely expressed in the membrane at densities below detectability with immunofluorescence. Triad targeting of GFP-I·II may have failed because this two-domain fragment expressed in the membrane lacked specific determinants of triad targeting present only in the fully assembled four-domain channel. In contrast, no charge movement was detected with III·IV expressed alone (ref. 16 and this study), indicating that this two-domain fragment was very poorly or not at all inserted into the membrane. Thus, targeting of III·IV had been hindered at an early step en route from the ER to the triad.

The Combination of the β-Interaction Domain and the Triad-Targeting Signal Is Not Sufficient for Correct Targeting of Individual Two-Domain Fragments. The finding that III·IV by itself is not targeted into the triad is in apparent conflict with a previous study by our laboratory in which we described a triad-targeting signal in the

Flucher et al.

C terminus (amino acids 1607–1661) of α_{1S} (11). The present data suggest that this targeting signal is not sufficient for triad targeting when contained in a half-channel construct rather than in the complete four-domain channel. This result did not come as a surprise, because earlier attempts in our laboratory to fuse the C terminus of α_{1S} onto an unrelated membrane protein, CD8, also failed to redirect CD8 into triads of dysgenic myotubes (B.E.F. and M.G., unpublished results). Thus, other parts of the channel must contribute to some aspect of triad targeting.

Because the β-interaction domain in the I–II loop has been shown to be crucially involved in the β-subunit-dependent release of channels from the ER (3), it was plausible to assume that the β-interaction domain and the C-terminal targeting motif might cooperate in consecutive steps of triad targeting. According to this model, an interaction of the β subunit with the I–II loop would be required for release of the channel from the ER and consequently allow membrane insertion. The C-terminal triad-targeting signal, on the other hand, would function in a consecutive step directing the α_1 subunit into the triad and/or in immobilizing it there (11). The observations that fragment I–II but not fragment III–IV produced intramembrane charge movement (ref. 16 and present study) are consistent with the idea that only I–II is inserted into the membrane but not into triads, because it contains the β-interaction domain and not the C-terminal triad-targeting motif. In contrast, the III–IV channel fragment, which lacks the β interaction domain, fails to be incorporated into the membrane because it is retained in the ER. Now the question is, would III–IV be targeted into triads if it had been inserted into the membrane?

Therefore we tested the hypothesis that the I–II loop and the C terminus may cooperate in triad targeting, by constructing and expressing composite two-domain Ca^{2+} channel fragments that contained both sequences. We fused the entire C terminus of α_{1S} onto GFP-I·II (GFP-I·II·tail) and we replaced in construct III·IV the loop connecting repeats III and IV with that connecting repeats I and II (III·IV·βin). Coexpression of these modified two-domain constructs with their normal complementary two-domain fragment (GFP-I·II·tail with III·IV, and III·IV·βin with GFP-I·II) restored normal Ca^{2+} currents and robust depolarization-induced Ca^{2+} transients (Table 2). This finding indicated that the modified two-domain fragments were normally expressed and could recombine into functional channels. Furthermore, in combination with their normal counterparts, both composite channel fragments were capable of being targeted into triads, although at a reduced rate. However, when expressed alone neither GFP-I·II·tail nor III·IV·βin was targeted into the triads (Table 1). Like their unmodified correlates, GFP-I·II·tail and III·IV·βin were never found colocalized with RyR1 clusters but were localized in the ER/SR system (Fig. 3). Finally, normal levels of charge movement could be recorded from GFP-I·II·tail (5.5 ± 1.8 nC/μF; $n = 7$) but not from III·IV·βin. Thus, the combination of the I–II loop, containing the β-interaction domain, and the C terminus, containing the triad-targeting signal, in either one of the two-domain Ca^{2+} channel constructs did not improve their triad targeting or membrane expression properties.

The poor ability of III·IV·βin to restore triad targeting in combination with GFP-I·II could be an indication that a compromised structure of the construct or the lack of the III–IV loop itself may have caused the failure to improve membrane expression. On the other hand, the possibility of a misfolded or damaged III·IV·βin is not supported by the normal restoration of EC coupling and current conduction observed upon coexpression with GFP-I·II. The discrepancy between poor restoration of triad targeting and efficient restoration of function by GFP-I·II + III·IV·βin can be explained by the different sampling used. Whereas with immunofluorescence the entire population of differently well developed myotubes in a sample is recorded,
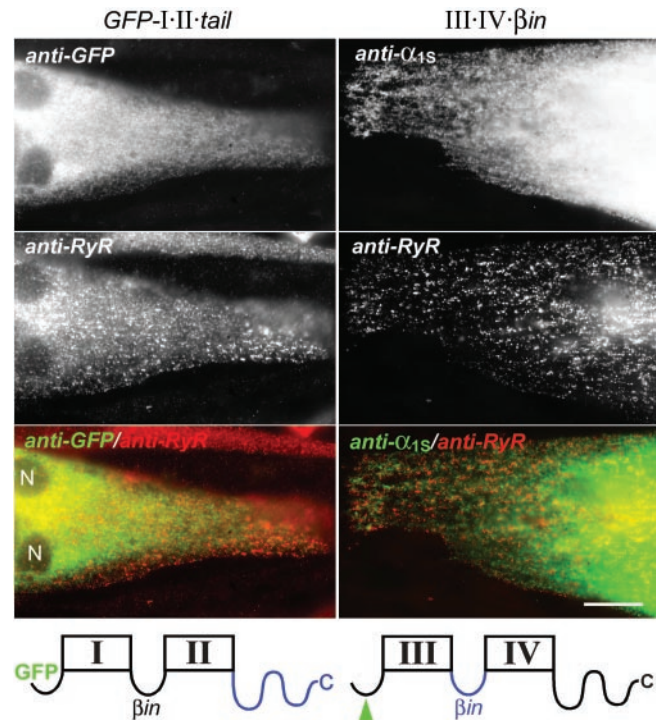
Fig. 3. Lack of triad targeting in two-domain Ca^{2+} channel constructs containing both the β-interaction domain of the I–II connecting loop and the C-terminal triad-targeting signal. Two-domain constructs containing both of these domains were generated by fusing the C terminus of α_{1S} onto GFP-I·II (GFP-I·II·tail) or by replacing the connecting loop between repeats III and IV by that between I and II (III·IV·βin) (blue sequences in the schematic drawings of transmembrane domain structures below the micrographs). Neither GFP-I·II·tail (*Left* column) nor III·IV·βin (*Right* column) was correctly localized in triad junctions (indicated by RyR clusters) when expressed individually in dysgenic myotubes. Merged color images (bottom row) of the micrographs above show the lack of colocalization of RyR clusters and Ca^{2+} channel constructs in the ER/SR network as distinct red and green labeling patterns, respectively. N, nuclei. (Scale bar, 20 μm.)

patch-clamp and Ca^{2+} release data are obtained only from well developed and strongly expressing myotubes. Recent data suggest that a specific cooperation of the β-interaction domain in the I–II loop with the III–IV loop is important for β-induced inactivation of the neuronal α_{1A} subunit (29). If the same principle would also apply to the possible role of β in the targeting of the α_{1S} subunit into skeletal muscle triads, this could explain why membrane insertion did not improve in III·IV·βin, in which the III–IV loop had been replaced by the I–II loop. However, GFP-I·II and GFP-I·II·tail, both of which contain the I–II loop but not the III–IV loop, were by themselves expressed in the membrane at normal levels. Thus, residues in the III–IV loop of α_{1S} appear not to be necessary for the putative role of β in membrane insertion in skeletal muscle cells.

In contrast to III·IV·βin, GFP-I·II·tail was expressed in the membrane but the addition of the entire C-terminal tail of α_{1S} did not result in triad targeting. Thus, the combination of the β-interaction domain and the C-terminal targeting signal is still not sufficient for triad targeting of a two-domain channel construct. Perhaps not only the presence but also the exact spatial arrangement of the two domains within the channel is important for their individual functions or their cooperation in triad targeting. However, Bichet *et al.* (3) were able to demonstrate specific effects of the β subunit in membrane targeting with the Ca^{2+} channel I–II loop fused to the C terminus of a K^+ channel. Apparently, this protein–protein interaction is not very

sensitive to the exact disposition of the β-interaction domain in the channel. Alternatively, other parts of the channel may also contribute to normal triad targeting. These could be overall structural determinants, such as the complete tertiary structure of the four-domain complex, or additional functional domains, such as another protein–protein interaction domain involved in the targeting process. Such features or sequences would most likely be conserved between differentially targeted Ca^{2+} channel isoforms, because exchanging domains other than the C terminus between α_{1S} and α_{1A} did not affect their targeting properties (11).

Whereas it is clear that both the β-interaction domain in the I–II loop and the targeting signal in the C terminus of α_{1S} play important roles in membrane expression and triad targeting of full-length Ca^{2+} channels, their joint actions are not sufficient to fully explain the targeting process in skeletal muscle. In contrast to membrane expression in heterologous expression systems, functional targeting of ion channels into specific membrane domains of differentiated cells seems to be a highly regulated mechanism involving multiple steps and protein domains. Here we show that the cooperation of the complementary halves of the Ca^{2+} channel α_{1S} subunit is necessary for triad targeting in skeletal muscle. The number, complete identity, and exact roles of the multiple domains of the α_{1S} subunit that contribute to this targeting function still remain elusive.

1. Catterall, W. A. (1995) *Annu. Rev. Biochem.* **64,** 493–531.
2. Pragnell, M., De Waard, M., Mori, Y., Tanabe, T., Snutch, T. P. & Campbell, K. P. (1994) *Nature (London)* **368,** 67–70.
3. Bichet, D., Cornet, V., Geib, S., Carlier, E., Volsen, S., Hoshi, T., Mori, Y. & De Waard, M. (2000) *Neuron* **25,** 177–190.
4. Gerster, U., Neuhuber, B., Groschner, K., Striessnig, J. & Flucher, B. E. (1999) *J. Physiol.* **517,** 353–368.
5. Neuhuber, B., Gerster, U., Döring, F., Glossmann, H., Tanabe, T. & Flucher, B. E. (1998) *Proc. Natl. Acad. Sci. USA* **95,** 5015–5020.
6. Nakai, J., Tanabe, T., Konno, T., Adams, B. & Beam, K. G. (1998) *J. Biol. Chem.* **273,** 24983–24986.
7. Grabner, M., Dirksen, R. T., Suda, N. & Beam, K. G. (1999) *J. Biol. Chem.* **274,** 21913–21919.
8. Catterall, W. A. (2000) *Annu. Rev. Cell Dev. Biol.* **16,** 521–555.
9. Peterson, B. Z., DeMaria, C. D., Adelman, J. P. & Yue, D. T. (1999) *Neuron* **22,** 549–558.
10. Walker, D., Bichet, D., Campbell, K. P. & De Waard, M. (1998) *J. Biol. Chem.* **273,** 2361–2367.
11. Flucher, B. E., Kasielke, N. & Grabner, M. (2000) *J. Cell Biol.* **151,** 467–478.
12. Proenza, C., Wilkens, C., Lorenzon, N. M. & Beam, K. G. (2000) *J. Biol. Chem.* **275,** 23169–23174.
13. Scott, V. E., Felix, R., Arikkath, J. & Campbell, K. P. (1998) *J. Neurosci.* **18,** 641–647.
14. Malouf, N. N., McMahon, D. K., Hainsworth, C. N. & Kay, B. K. (1992) *Neuron* **8,** 899–906.
15. Wielowieyski, P. A., Wigle, J. T., Salih, M., Hum, P. & Tuana, B. S. (2001) *J. Biol. Chem.* **276,** 1398–1406.
16. Ahern, C. A., Arikkath, J., Vallejo, P., Gurnett, C. A., Powers, P. A., Campbell, K. P. & Coronado, R. (2001) *Proc. Natl. Acad. Sci. USA* **98,** 6935–6940.
17. Grabner, M., Dirksen, R. T. & Beam, K. G. (1998) *Proc. Natl. Acad. Sci. USA* **95,** 1903–1908.
18. Horton, R. M., Hunt, H. D., Ho, S. N., Pullen, J. K. & Pease, L. R. (1989) *Gene* **77,** 61–68.
19. Powell, J. A., Petherbridge, L. & Flucher, B. E. (1996) *J. Cell Biol.* **134,** 375–387.
20. Flucher, B. E., Andrews, S. B., Fleischer, S., Marks, A. R., Caswell, A. & Powell, J. A. (1993) *J. Cell Biol.* **123,** 1161–1174.
21. Morton, M. E. & Froehner, S. C. (1987) *J. Biol. Chem.* **262,** 11904–11907.
22. Giannini, G., Conti, A., Mammarella, S., Scrobogna, M. & Sorrentino, V. (1995) *J. Cell Biol.* **128,** 893–904.
23. Adams, B. A., Tanabe, T., Mikami, A., Numa, S. & Beam, K. G. (1990) *Nature (London)* **346,** 569–572.
24. El-Hayek, R., Antoniu, B., Wang, J., Hamilton, S. L. & Ikemoto, N. (1995) *J. Biol. Chem.* **270,** 22116–22118.
25. Flucher, B. E., Phillips, J. L., Powell, J. A., Andrews, S. B. & Daniels, M. P. (1992) *Dev. Biol.* **150,** 266–280.
26. Stühmer, W., Conti, F., Suzuki, H., Wang, X. D., Noda, M., Yahagi, N., Kubo, H. & Numa, S. (1989) *Nature (London)* **339,** 597–603.
27. Kozak, M. (1984) *Nucleic Acids Res.* **12,** 857–872.
28. Wilkens, C. M., Kasielke, N., Flucher, B. E., Beam, K. G. & Grabner, M. (2001) *Proc. Natl. Acad. Sci. USA* **98,** 5892–5897.
29. Geib, S., Sandoz, G., Mabrouk, K., Matavel, A., Marchot, P., Hoshi, T., Villaz, M., Ronjat, M., Miquelis, R., Leveque, C. & De Waard, M. (2002) *Biochem. J.* **364,** 285–292.